

Magnetic Measurements of the Fermilab High Gradient Quadrupoles for the LHC Interaction Regions

R. Bossert, J. Brandt, J. DiMarco, M.J. Lamm, F. Nobrega,
G. Sabbi, P. Schlabach, C. Sylvester, M. A. Tartaglia, J. C. Tompkins, A.V. Zlobin,
Fermilab, Batavia, Illinois, USA;

S. Caspi,
Lawrence Berkeley National Laboratory, Berkeley, California, USA

Abstract—Three short models of the MQXB quadrupole magnet for the LHC interaction regions have been built and tested at Fermilab. In this paper we present the magnetic field measurement results and compare them with expectations based on as-built dimensional parameters and with a preliminary table of field quality requirements.

I. INTRODUCTION

The MQXB design is based on a 2-layer, $\cos(2\theta)$ coil (Fig. 1) operating in superfluid helium at 1.9 K [1]. A magnet model program aimed at validating and optimizing this design is under way. The first three 2 m long model magnets, HGQ01, HGQ02, and HGQ03, have been tested in the Fermilab Vertical Magnet Test Facility from February to August of this year. In this paper, measurements of the magnetic field of the three models are discussed and compared with calculations [2].

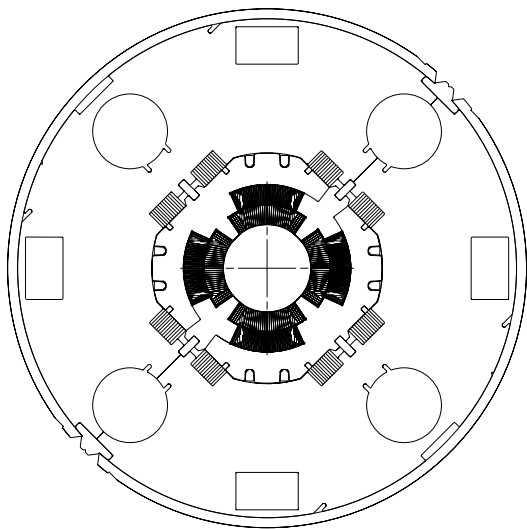


Fig. 1. HGQ cross-section.

A rectangular coordinate system is defined with the z axis at the center of the magnet aperture and pointing from the return end towards the lead end, the x axis horizontal and pointing to the right of an observer who faces the magnet from the lead end, the y axis vertical and

pointing upwards. The field is represented in terms of harmonic coefficients defined by the power series expansion

$$B_y + iB_x = B_2 10^{-4} \sum_{n=1}^{\infty} (b_n + ia_n) \left(\frac{x + iy}{r_0} \right)^{n-1}$$

where B_x and B_y are the field components, B_2 is the quadrupole field, b_n and a_n are the $2n$ -pole coefficients ($b_2=10^4$). The reference radius r_0 is 17 mm [3].

We begin with a description of the system used for magnetic measurements. This is followed by presentation of field measurements and comparison to calculated values and a preliminary field specification. We then turn to detailed comparisons of measured and calculated fields for various topics of interest.

II. MEASUREMENT SYSTEM

Magnetic measurements presented in this paper were performed using a vertical drive, rotating coil system obtained from the SSCL [4]. For measurements of HGQ01, we used the rotating coil from this system which has 5 windings on a machined ceramic probe form: tangential, 2 dipole bucking, and 2 quadrupole bucking windings. The probe has nominal diameter 25.4 mm and length 25 cm. A new probe optimized for 70 mm aperture magnets was commissioned for the HGQ02 test. It has 40.6 mm nominal diameter and length 82 cm wound on a machined G10 form. The winding design is similar to that of the SSCL probe. Improvements to the probe support in the warm finger and to the system driveshaft were also made. Coil winding voltages are read out using 5 HP3458 DVMs. An additional DVM is used to monitor magnet current. The DVMs are triggered simultaneously by an angular encoder on the probe shaft, synchronizing measurements of field and current. Feed down of the quadrupole signal to the dipole is used to center the probe in the magnet.

As customary for LHC magnets, field harmonics will be expressed in “units” of 10^{-4} of the main field component at a reference radius of 17 mm.

III. FIELD QUALITY ANALYSIS

A comparison between the body harmonics measured in the three models is shown in Table I. These data are published here in the same reference frame and for measurements made in a similar fashion. Improvements of

TABLE I
FIELD HARMONICS MEASURED AT MAGNET CENTER AT 6 KA.

n	Normal (b_n)			Skew (a_n)		
	01	02	03	01	02	03
HGQ						
3	0.36	-0.70	1.04	0.27	0.55	-0.30
4	0.26	0.18	0.14	2.00	0.53	0.32
5	-0.29	0.09	-0.34	0.02	-0.17	0.26
6	-3.91	-1.54	-1.02	-0.08	0.03	0.07
7	-0.08	-0.01	-0.06	-0.05	0.00	-0.03
8	0.06	0.01	0.00	0.02	0.02	0.03
9	0.04	0.00	0.00	0.01	-0.01	0.01
10	-0.10	-0.10	-0.04	0.02	0.00	-0.01

TABLE II
COMPARISON OF MEASURED AND CALCULATED HARMONICS IN THE MAGNET STRAIGHT SECTION.

n	HGQ01		HGQ02		HGQ03	
	calc.	meas.	calc.	meas.	calc.	meas.
b_6	-4.24	-3.91	-2.86	-1.54	-1.39	-1.02
b_{10}	-0.14	-0.10	-0.09	-0.10	-0.04	-0.04
a_4	1.27	2.00	0.94	0.53	0.00	0.32
a_8	0.02	0.02	0.00	0.02	0.00	0.03

the field quality have been obtained by optimizing the coil fabrication procedure [5]. The coil shim thickness used in fabricating HGQ02 was reduced by a factor of 2 from that of HGQ01 by adjusting the cable insulation scheme and the coil curing procedure and reduced even more in HGQ03 with corresponding improvements in the field quality. Measured values for the “allowed” harmonic components can be compared to calculations. This comparison is given in Table II for the 3 magnets.

The measured harmonics can also be compared to the preliminary field quality specification for MQXB magnets [6] which have been established to provide a common reference for the discussion of field quality issues. Expected values of the mean, uncertainty in mean and standard deviation are listed in Table III for each harmonic component. The results of magnetic measurements show that the required low systematic values of field harmonics in the magnet body can be achieved within specified uncer-

TABLE III
MQXB REFERENCE HARMONICS [6].

n	$\langle b_n \rangle$	$d(b_n)$	$\sigma(b_n)$	$\langle a_n \rangle$	$d(a_n)$	$\sigma(a_n)$
Straight section						
3	0.0	0.34	0.85	0.0	0.34	0.85
4	0.0	0.26	0.87	0.0	0.26	0.87
5	0.0	0.20	0.34	0.0	0.20	0.34
6	0.0	0.17	0.25	0.0	0.17	0.25
7	0.0	0.14	0.11	0.0	0.14	0.11
8	0.0	0.10	0.07	0.0	0.10	0.07
9	0.0	0.08	0.07	0.0	0.08	0.07
10	0.0	0.06	0.03	0.0	0.06	0.03
Lead end (magnetic length 0.41 m)						
2	-	-	-	38	0.0	0.0
6	5.5	0.0	0.0	0.2	0.0	0.0
10	-0.2	0.0	0.0	-0.1	0.0	0.0
Return end (magnetic length 0.33 m)						
6	1.2	0.0	0.0	0.0	0.0	0.0
10	-0.3	0.0	0.0	0.0	0.0	0.0

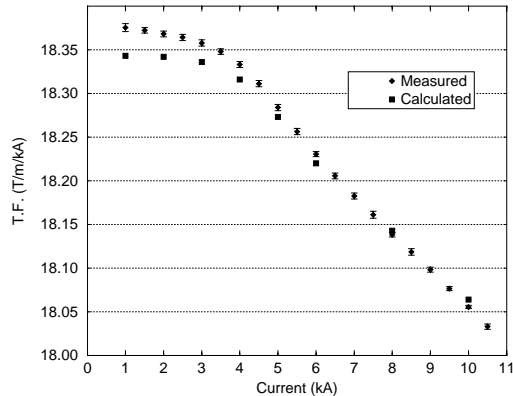


Fig. 2. Magnet transfer function of HGQ01.

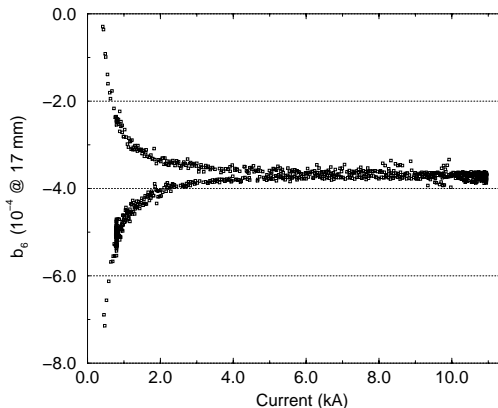


Fig. 3. Normal dodecapole (units at a reference radius of 17 mm) in HGQ01 vs. current.

tainty with little or no magnet cross section correction. The observed RMS spread in harmonics for three short models is within the range specified.

Magnet transfer function (G/I) at low currents is 18.37 T/m/kA (Fig. 2). Due to iron saturation, a 2% decrease is observed in the current range 1-11 kA. The nominal current for MQXB is 0.8 kA at injection, 11.1 kA in collision. Good agreement is found between measured values and design calculations.

Fig. 3 shows the dependence of the normal dodecapole on current in HGQ01. At low ramp rates, the mean of up and down ramps reflects the contributions of iron saturation and conductor displacement under Lorentz forces, while the difference between mean values and up-down ramps is due to persistent currents in the superconducting coil. The observed change in the mean b_6 is very small over the entire current range and in good agreement with design calculations, as shown in Fig. 4. The persistent current b_6 at injection is less than 1 unit. The dependence of b_{10} on current is shown in Fig. 5. The plot contains 3 ramp cycles of which the first is noticeably different. The second and third, corresponding to normal operation, are identical and show very little dependence on current. The differences between the harmonics mea-

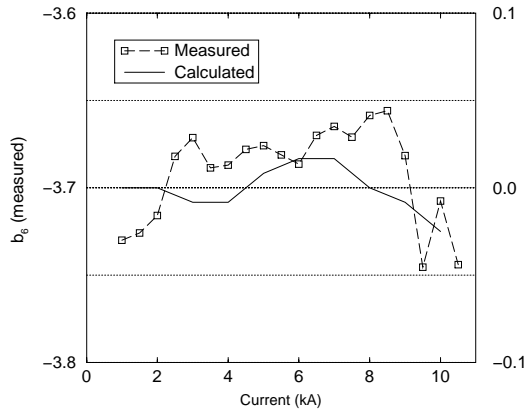


Fig. 4. Measured normal dodecapole (units at a reference radius of 17 mm) in HGQ01 vs. current compared to calculations.

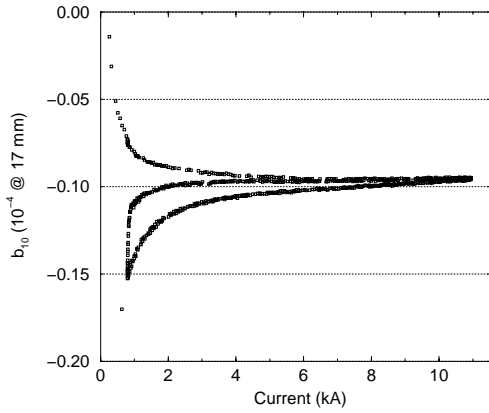


Fig. 5. Normal 20-pole (units at a reference radius of 17 mm) vs. current in HGQ02.

sured during up and down ramp for two different ramp rates is summarized in Table IV. The differences between up and down ramp are small.

As part of the normal testing cycle, the field is measured

TABLE IV

DIFFERENCES BETWEEN THE FIELD AT 6 kA MEASURED ON THE UP AND DOWN RAMP. DIFFERENCES GREATER THAN 0.01 UNIT ARE GIVEN.

n	HGQ01		HGQ02		HGQ03	
	10 A/s	80 A/s	10 A/s	80 A/s	10 A/s	80 A/s
b_3	-	-	0.01	-0.03	-	-0.01
b_4	-	-	0.01	-0.01	-	0.02
b_5	-	-	-0.03	-0.04	-	-0.01
b_6	-0.12	-0.08	-0.19	-0.26	-0.12	-0.19
b_7	-	-	-	-0.01	-	-0.01
b_9	-	-	-0.01	-0.01	-	-
b_{10}	-	-	0.01	0.01	-	0.01
a_3	-	-	0.01	0.04	-	-0.02
a_4	0.07	0.25	-	-0.03	-	0.01
a_5	-	-	0.02	0.03	-	0.02
a_6	-	-	0.01	0.01	-	0.01
a_7	-	-	-	-0.01	-	-0.01
a_9	-	-	-	0.01	-	-

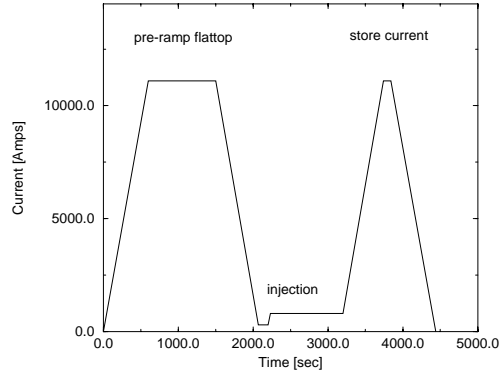


Fig. 6. Current vs. time during a typical accelerator cycle.

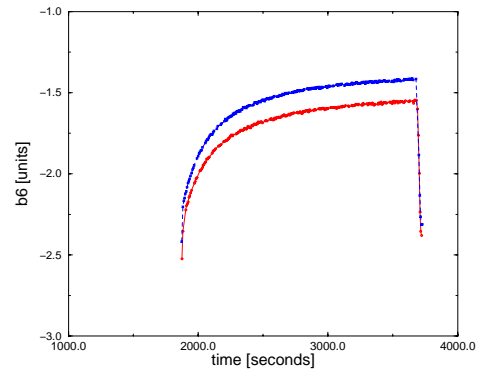


Fig. 7. Dodecapole (units at a reference radius of 17 mm) in HGQ02 as a function of time during the injection plateau for two different pre-cycle currents (9 and 11 kA).

during a pseudo-accelerator cycle (Fig. 6) in which the magnet is ramped through a series of pre-cycles, brought to injection current and held, then ramped to flat top. Fig. 7 shows the change in b_6 during a 30 min. injection plateau measured in HGQ02. Table V summarizes the change in field harmonics at injection measured in the three magnets in terms of slope fit to the harmonic as a function of log-time. With the exception of b_4 and

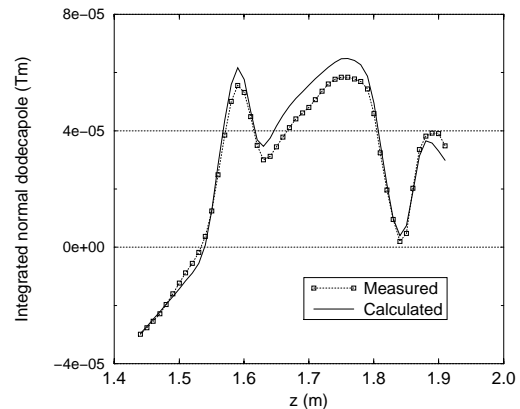


Fig. 8. Normal dodecapole in HGQ01 lead end.

TABLE V
SUMMARY OF FIELD HARMONICS CHANGES DURING THE INJECTION PLATEAU. VALUES ARE SLOPE FROM A FIT OF THE HARMONIC AS A FUNCTION OF LOG-TIME FROM T=100 TO T=1000 SEC. T=0 IS DEFINED BY THE FIRST POINT AT INJECTION CURRENT.

n	HGQ01	HGQ02	HGQ03
b_3	0.048	-0.008	-0.040
b_4	-0.218	-0.018	-0.019
b_5	0.077	-0.011	-0.001
b_6	0.085	0.384	0.103
b_7	0.035	0.003	-0.000
b_8	0.016	-0.001	-0.004
b_9	-0.002	0.002	-0.000
b_{10}	-0.022	0.011	0.008
a_3	-0.096	-0.015	0.018
a_4	-0.363	0.025	0.020
a_5	-0.069	0.006	-0.008
a_6	-0.028	0.013	0.008
a_7	-0.006	-0.003	-0.006
a_8	0.024	0.002	0.000
a_9	-0.001	0.000	-0.000
a_{10}	-0.004	-0.000	-0.000

TABLE VI
COMPARISON OF MEASURED AND CALCULATED HARMONICS IN THE MAGNET LEAD END (INTEGRATION INTERVAL [1.31, 2.03] FOR HGQ01, [1.29, 2.11] FOR HGQ02 AND HGQ03).

n	HGQ01		HGQ02		HGQ03	
	calc.	meas.	calc.	meas.	calc.	meas.
b_6	3.1	2.9	5.5	4.2	5.4	3.8
b_{10}	-0.3	-0.3	-0.3	-0.2	-0.4	-0.4
a_6	0.5	0.1	0.4	0.2	-0.1	-0.3
a_{10}	-0.1	-0.1	0.0	0.0	0.0	0.0

a_4 (HGQ01) and b_6 , the change in field during injection is small. Observation of larger changes in a_4 and b_6 is not so surprising, as these are the largest observed harmonics (Table I). The change in b_4 is not so easily explained. The observed difference in the slope of b_6 from magnet to magnet may be due to changes in coil fabrication procedures and splice configuration. Note that, while we have observed and are reporting on these dynamic effects, they have negligible impact on machine performance as the number of insertion quadrupoles is a small fraction

of all magnets.

Magnetic measurements of the magnets were made at a series of positions along the z axis. A scan was made of the entire magnet length along with a scan of the lead end region with smaller step sizes. A comparison of measured and calculated harmonics for allowed values in the magnet lead end is given in Table VI. A comparison of normal and measured dodecapole (units at a reference radius of 17 mm) as a function of z in the lead end is plotted in Fig. 8. Values given are integrated over the length of the 25 cm probe. Both the integrated field values and the shape show good agreement between measurement and calculation.

IV. CONCLUSIONS

Magnetic measurements of the HGQ models confirm design calculations. There is good agreement between measured and calculated geometric harmonics, magnetization and Lorentz force effects. Measurement of the field along the magnet length and in the magnet end region also agree well with calculated values.

Refinements in magnet fabrication have significantly improved the field quality. Measurements of the first 3 magnets confirm that the straight section harmonics are within the uncertainty specified in the MQXB reference harmonics table (Table III). The spread in measured harmonics is within the range specified. Systematic errors in the end design are expected to be substantially reduced after end field optimization [7].

REFERENCES

- [1] R. Bossert, et al., Proc. MT-15 Conf., October 1997.
- [2] G. Sabbi, et al., Proc. MT-15 Conf., October 1997.
- [3] L. Walckiers, P. Lefevre, LHC-MTA/LW, April 1998.
- [4] G. Ganetis, et al., Proc. PAC-87 Conf., March 1987.
- [5] R. Bossert et al., "Design, Development and Test of 2m Quadrupole Model Magnets for the LHC Inner Triplet", Paper LKA-01 this Conference.
- [6] W. Chou, et al., Fermilab Pub-97/378, November 1997.
- [7] G. Sabbi, Fermilab TD-98-037, May 1998.